A Novel High-Gain Tetrahedron Origami

Syed Imran Hussain Shah, Dongju Lee, Manos M. Tentzeris, *Fellow, IEEE*, and Sungjoon Lim, *Member, IEEE*

***Abstract*—In this letter, a novel high-gain tetrahedron origami antenna is introduced. The antenna comprises a triangular-shaped monopole, a reflector, and two parasitic strip directors on a paper substrate. The directors and the reflector are employed to increase the antenna gain. The step-by-step origami folding procedure is presented in detail. The proposed design of antenna is verified by both simulations and measurements with a fabricated prototype. The antenna exhibits a 10-dB impedance bandwidth of 66% (2–4 GHz) and a peak gain of 9.5 dBi at 2.6 GHz.**

***Index Terms*—Directional antenna, director, high-gain antenna, origami antenna, tetrahedron.**

I. Introduction

ORIGAMI is a Japanese word meaning "paper folding." The associated concept has been used in many areas such as biochemistry, robotics, energy harvesting, architecture, medical devices, and spaceborne applications [1]. Its folding and unfolding capabilities can present significant advantages in electromagnetic (EM) applications. For instance, multifunctionality can be achieved by folding and unfolding while reducing payload costs and overall volume [2]. Easy and fast designing procedures are additional benefits of origami antennas.

Very few examples of antennas and RF circuits designed with the origami concept can be found in the literature. One of them is a 3-D origami antenna designed in an accordion shape, proposed in [3]. Different ways of folding and unfolding operations can change the height of the antenna, and thus reconfigure its frequency characteristics. In [4], a frequency- and mode-reconfigurable quadrifilar helical origami antenna is presented. In [5], an origami antenna is designed based on an origami spring structure and the antenna. The antenna height is controlled by pressing the spring base. In [6], an origami Yagi antenna is designed for spaceborne applications, but the antenna can only be folded using a servo motor. One of the well-known approaches to obtain a relatively higher gain is the use of antenna arrays, in which a number of antennas are appropriately arranged.

A common drawback of this technique is the associated level of losses in the resulting complicated feed network [7]. In [8], a high-gain antenna is implemented with a stub-loaded monopole that features the large length of 100 mm over an infinite ground. In [9], a high-gain antenna is obtained with a combination of a substrate integrated waveguide (SIW) and metamaterial technologies. An artificial magnetic conductor is used for gain enhancement in [10]. In [11], a high-gain antenna is presented, which uses stacked rings based on low-temperature cofired ceramic (LTCC) multilayer technology. Metal-stacked rings are used as directors to increase the antenna gain. Complementary electromagnetic band-gap (EBG) structures have also been used to improve the gain of antennas [12], with EBG geometries of square and circular shapes being implemented with and without vias. In [13], a high-gain antenna is realized by using frequency selective reflectors (FSRs). The FSRs are installed at a height of 49.6 mm on the large size ground plane. In [14], a high-gain quasi-Yagi antenna is designed by using a parabolic reflector.

In this letter, a high-gain tetrahedron origami antenna is presented. The proposed antenna has high gain, a significantly more wideband (66%) impedance bandwidth, and low cost, is simple, and can be easily fabricated using fast manufacturing technologies. The presented antenna consists of a triangular-shaped monopole, a reflector, and two parasitic strip directors. Two directors and a reflector play an important role to increase antenna's gain. A detailed step-by-step origami folding procedure for the proposed antenna—which covers the 2–4-GHz frequency range, with a measured peak gain of 9.5 dBi—is presented.

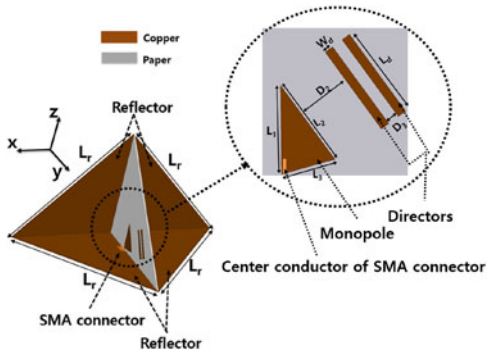

Fig. 1. Geometry of tetrahedron origami antenna: $L_1 = 31$, $L_2 = 32$, $L_3 = 20$, $L_d = 36$, $W_d = 3.8$, $D_1 = 38.5$, $D_2 = 20.5$, $D_3 = 6$, $L_r = 193$, $L_g = 193$ (units: millimeters).

II. Origami Antenna Design

For proof-of-concept purposes, the proposed antenna is designed on a paper substrate in an origami tetrahedron shape, as presented in Fig. 1. It consists of a triangular-shaped monopole (the driven element), a reflector, and two directors. The triangular shape of the driven element and the position of the directors are chosen to connect the axis of the driven element and directors and to separate the directors by a certain distance from the reflector.

Manuscript received July 14, 2016; accepted September 13, 2016. Date of publication September 15, 2016; date of current version April 10, 2017. This work was supported in part by the Chung-Ang University Research Grants in 2015 and in part by the Ministry of Science, ICT and Future Planning, South Korea, under the Information Technology Research Center support program (IITP-2016-H8501-16-1007) supervised by the Institute for Information & Communications Technology Promotion.

S. I. H. Shah, D. Lee, and S. Lim are with the School of Electrical and Electronics Engineering, College of Engineering, Chung-Ang University, Seoul 156-756, South Korea (e-mail: engr.shahsyedimran@gmail.com; dongju0721@daum.net; sungjoon@cau.ac.kr).

M. M. Tentzeris is with the School of Electrical and Computer Engineering, College of Engineering, Georgia Institute of Technology, Atlanta, GA 30332 USA (e-mail: etentze@ece.gatech.edu).

Color versions of one or more of the figures in this letter are available online at http://ieeexplore.ieee.org.

Digital Object Identifier 10.1109/LAWP.2016.2609898

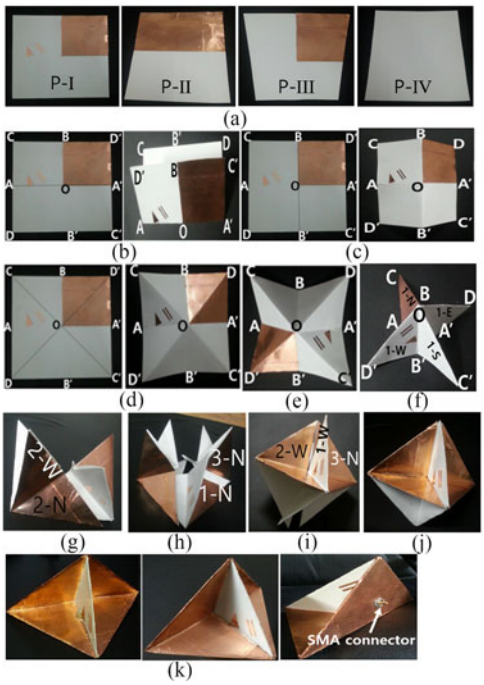

Fig. 2. Origami setup. (a) Four paper sheets. (b) Step 1a: folding and unfolding along AA′. (c) Step 1b: folding and unfolding along BB′. (d) Step 1c: folding and unfolding along CC′ and DD′. (e) Creased sheet. (f) Step 1d: folding for complete star. (g) Step 3a: joining stars #1 and #2. (h) Step 3b: joining star #3. (i) Three joined stars #1, #2, and #3. (j) After joining star #4. (k) Antenna prototype top view. (k) Antenna prototype front view, side view, and back view.

The origami antenna design and folding process can be divided in several steps, as presented in Fig. 2. First, four different square paper sheets with the same area ($270 \times 270\,\text{mm}^2$) and a thickness of 0.25 mm are taken. These paper sheets are labeled I–IV. Second, sheet I is selected as the substrate for the driven triangular patch realized with a copper film tape, as well as for the two antenna directors realized with two similar copper strips with dimensions of $36 \times 3.8\ \text{mm}^2$. A $135 \times 135\text{-mm}^2$ copper film tape is attached on a quarter-section of sheet I (top right, next to the top left quarter including the driven antenna and the director elements) to serve as the reflector for the antenna. The conductivity of copper film is $4.4 \times 10^5\ \text{S/m}$ [15], which is lower than the conductivity of regular copper, which is $5.96 \times 10^7\ \text{S/m}$ [16].

As a first step, P-I in Fig. 2(a) is marked with the segments AA′, BB′, CC′, DD′, and the center point O; CC′ and DD′ are diagonals; AA′ and BB′ are the horizontal and vertical median lines. In step 1a, P-I is folded and unfolded across AA′, as shown in Fig. 2(b). This creates a crease dividing the paper to two half-sections. In step 1b, the sheet is folded and unfolded along BB′ to add a second crease; the two creases now divide the square sheet into quarters. In step 1c, the sheet is folded and unfolded across CC′ and DD′, as represented by the dotted lines in Fig. 2(d). These steps do therefore create creases dividing the paper sheet into eight triangular sections, as presented in Fig. 2(e). Folding A and A′ toward B and B′ (step 1d), P-I becomes star-shaped, and its four arms are indicated as 1-N (north), 1-S (south), 1-E (east), and 1-W (west) as shown in Fig. 2(f).

In a second step, P-II, P-III, and P-IV in Fig. 1(a) are utilized. Two copper films with different dimensions ($270 \times 135\,\text{mm}^2$ and $135 \times 135\,\text{mm}^2$) are attached to one half-section of P-II and a quarter-section of P-III, respectively, to serve as the reflector in the final antenna design. Steps 1a–d are then repeated with P-II, P-III, and P-IV, resulting in three additional stars. At the end of step 2, we will therefore have four different stars, which can be labeled as stars #1, #2, #3, and #4 for P-I, P-II, P-III, and P-IV, respectively.

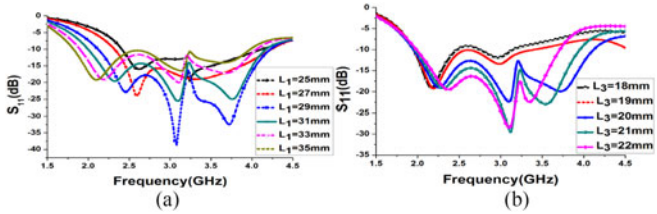

Fig. 3. Simulated reflection coefficients at different (a) L_1 and (b) L_3.

In a third step, stars #1, #2, #3, and #4 are joined and glued. As shown in Fig. 2(g), 1-S arm of star #1 is inserted into 2-N slot of star #2. Next, 3-W arm of star #3 is inserted into 1-N slot of star #1 as shown in Fig. 2(h). Three arms of star #4 are inserted into three slots of stars #1, #2, and #3 as shown in Fig. 2(i). For instance, 4-S arm of star #4 is inserted into 1-W slot of star #1 where the monopole and directors are realized. 4-W and 4-E arms of star #4 are inserted into 2-W slot of star #2 and 3-N slot of star #3, respectively, where the reflector is realized.

The tetrahedron origami antenna is then completed by cutting unnecessary paper (bottom half) from the composite prototype presented in Fig. 2(j). The resulting antenna prototype is displayed in Fig. 2(k).

The antenna is excited via a 50-Ω subminiature-version-A (SMA) connector. The inner pin of the SMA connector is connected to the triangular-shaped monopole as shown in Fig. 1. The outer ground of the SMA connector is connected to the reflector as shown in Fig. 2(k).

The proposed antenna is simulated and analyzed using the ANSYS High Frequency Structure Simulator. The utilized paper substrate is modeled in the simulations with a relative permittivity ε_r of 2.2 and a dielectric loss tangent of 0.02. In the simulation, the antenna is first designed around the center frequency of 2.6 GHz without the reflector, then the reflector is added to increase antenna's peak gain. The two directors are also added, to further increase antenna's peak gain. Fig. 3 shows the parametric study for the dimensions of the triangular monopole. In Fig. 3(a), the reflection coefficients are plotted by varying L_1 from 25 to 35 mm while L_3 is fixed at 21 mm. As L_1 is increased from 25 to 31 mm, impedance bandwidth increased, but further increase in L_1 deteriorates impedance matching. Therefore, $L_1 = 31$ mm is selected to achieve impedance matching over 2–4 GHz. In Fig. 3(b), the reflection coefficients are shown by varying L_3 from 18 to 22 mm. As L_3 is increased from 18 to 20 mm, impedance bandwidth increases. However, further increase in L_3 decreases the impedance bandwidth. Therefore, $L_3 = 20$ mm is selected for the triangular monopole design. Finally, the optimized dimensions of the three sides of the triangular monopole are $L_1 = 31$ mm, $L_2 = 32$ mm, and $L_3 = 20$ mm.

Distance between the triangular monopole and reflector (D_1) is determined after considering directivity. Fig. 4 shows the simulated peak gain versus at different D_1. At $D_1 = 38.5$ mm, the peak gain is 8.4 dBi, which is the highest peak gain with the reflector. As shown in Fig. 5(a) and (b), the reflector increases the peak gain from 4.6 to 8.4 dBi.

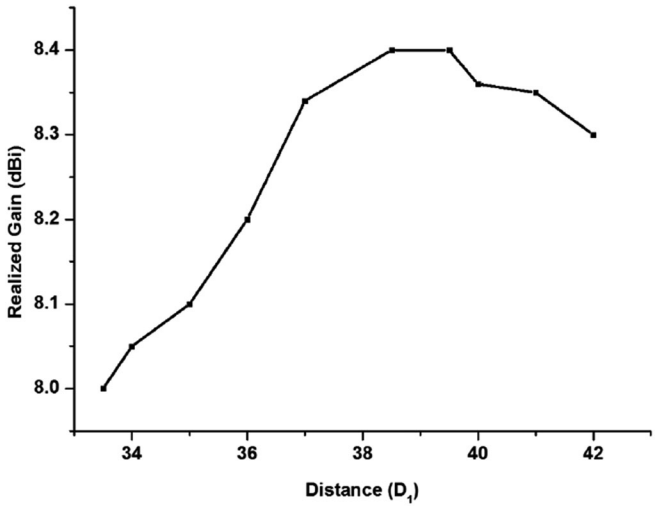

Fig. 4. Simulated peak gain versus different D_1 (mm).

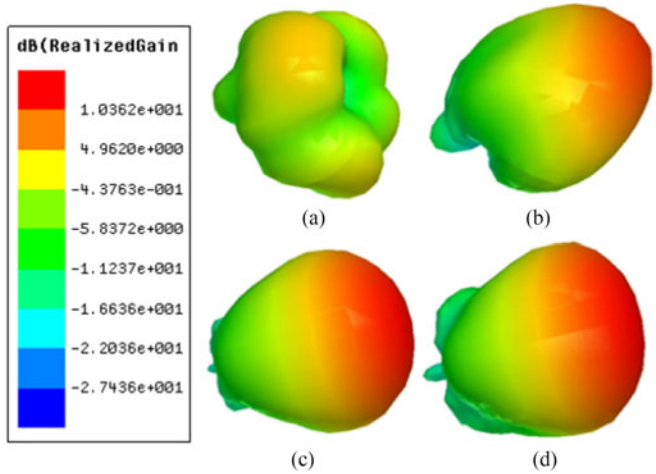

Fig. 5. Simulated 3-D radiation patterns at 2.6 GHz. (a) Without the reflector and director. (b) With the reflector and without directors. (c) With the reflector and one director. (d) With reflector and two directors.

Fig. 5 shows the simulated 3-D radiation patterns of the antenna at 2.6 GHz. In order to further increase directivity, directors are employed. Its length (L_d) and width (W_d) are 36 and 3.8 mm, respectively. Similarly, the distance between the triangular monopole and director (D_2) and the distance between each director (D_3) are optimized to achieve the highest peak gain. In addition, the number of the directors is increased to achieve higher peak gain. Fig. 6 shows the antenna's peak gain as a function of the number of directors (with equal spacing). As shown, the antenna gain is maximized for two directors. When additional directors are added, the antenna gain decreases. Fig. 5(c) and (d) shows the simulated 3-D radiation patterns of the antenna with one and two directors, respectively. Finally, D_2 and D_3 are determined to be 20.5 and 6 mm, respectively. The peak gain of the final antenna design is increased up to 10.3 dBi. The antenna maximum radiation direction is at an elevation angle (θ) of 60°.

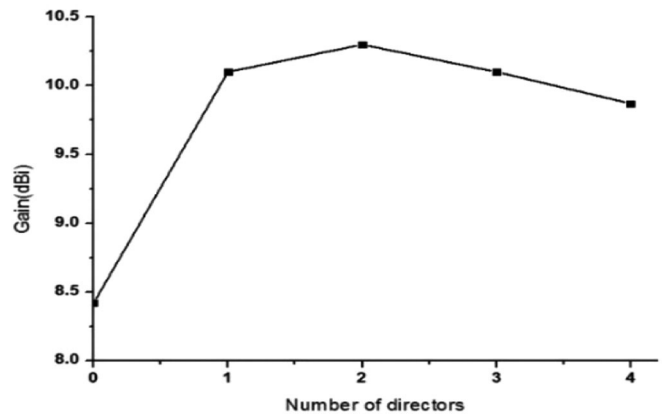

Fig. 6. Simulated peak gain versus the number of directors.

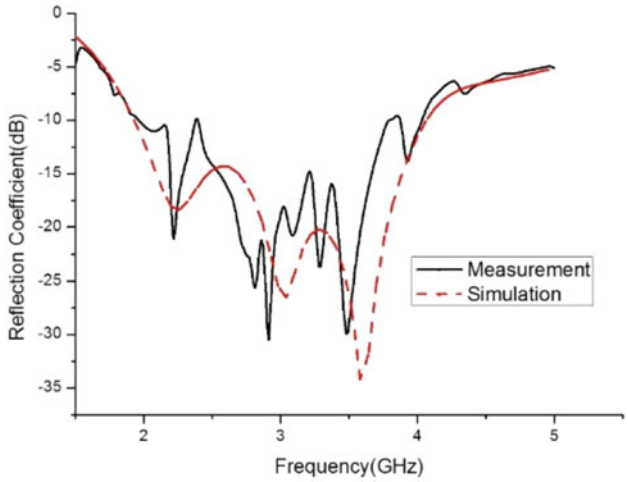

Fig. 7. Simulated and measured reflection coefficients of the proposed origami antenna.

III. Measurement Results

An antenna prototype was built on paper substrate in an origami tetrahedron shape, and shown in Fig. 2(k). The reflection coefficient of the antenna was measured with an Anritsu MS2038C vector network analyzer. In Fig. 7, both the simulated and measured reflection coefficients of the antenna are shown. These reflection coefficients show a –10-dB impedance bandwidth of 66% covering the 2–4-GHz frequency range.

There is a slight difference between the simulated and measured reflection coefficients, most likely due to minor fabrication and folding errors. However, both still show almost the same –10 dB impedance bandwidth. A comparison between the simulated and measured radiation patterns is presented in Fig. 8, for frequencies of 2, 2.6, 3.2, and 3.8 GHz. As shown, the main beam is directed toward $\theta = 60°$, because of the axis connecting the driven antenna and directors. The simulated and measured patterns show very good agreement at 2 and 2.6 GHz. However, the discrepancy between the simulated and measured patterns is observed at 3.2 and 3.8 GHz because permittivity and tangential loss of paper are characterized at 2 GHz. EM parameters of paper are changed as frequency increases. In addition, the assembly errors are more sensitive in high frequencies.

In Fig. 9, the simulated and measured peak gains are plotted as a function of frequency. At 2.6 GHz, the measured peak gain is

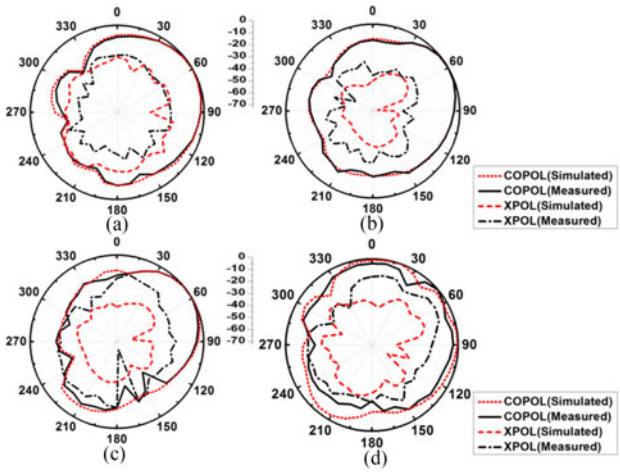

Fig. 8. Simulated and measured normalized radiation patterns on the *yz*-plane. (a) 2 GHz. (b) 2.6 GHz. (c) 3.2 GHz. (d) 3.8 GHz.

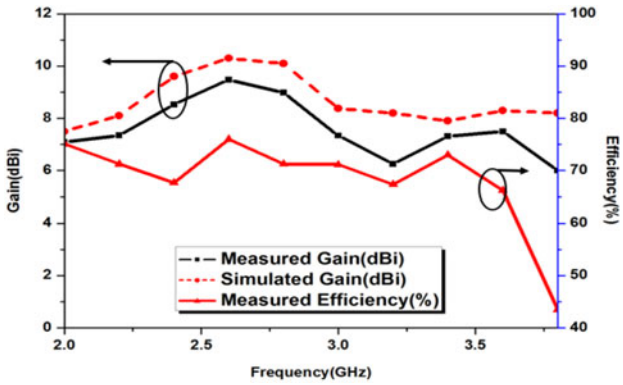

Fig. 9. Simulated and measured peak gain and efficiency as a function of frequency.

TABLE I
PERFORMANCE COMPARISON OF THE PROPOSED ANTENNA TO PREVIOUSLY PROPOSED HIGH-GAIN ANTENNAS

Proposed in	Frequency (GHz)	10 dB BW (%)	Peak gain (dBi)	Technology
[9]	4.95–5.00	1.2	8	Stub-loaded monopole
[10]	5.58–6.03	9	10	SIW + Metamaterial
[11]	1.84–2.05	10.8	12.45	AMCs
[12]	36.0–37.2	3.2	8.1	LTCC
[13]	7.80–8.10	5	8.4	EBG
[14]	1.65–2.3	33	11.8	FSR
[15]	2.28–2.63	14	6.5	Parabolic reflector
This study	2.00–4.00	66	9.5	Origami

BW: bandwidth; AMCs: artificial magnetic conductors; LTCC: low-temperature cofired ceramic multilayer; EBG: electromagnetic band-gap; FSR: frequency selective reflectors.

9.5 dBi, which is lower than the simulated peak gain of 10.3 dBi because of dielectric loss from glues. In addition, it is observed from Fig. 9 that the measured efficiency at 2.6 and 3.8 GHz is 76% and 43.5%, respectively.

In Table I, the performance of the proposed antenna is compared to those of other high-gain antennas [9]–[15]. In addition to its high gain, the proposed antenna shows features a much wider (by almost one order of magnitude) –10-dB impedance bandwidth. The manufacturing procedure of the proposed antenna is much simpler and easier than those of the other high-gain antennas, while the proposed antenna has very low cost, as it can be easily fabricated on paper substrates.

IV. CONCLUSION

A novel high-gain tetrahedron origami antenna is introduced in this letter. The antenna has an impedance bandwidth of 66% (2–4 GHz) and a peak gain of 9.5 dBi at 2.6 GHz. Being designed on a paper substrate, the proposed antenna is very low-cost. The antenna origami-manufacturing procedure is very easy and fast as it can be realized by just folding paper substrates. In spite of 3-D configuration, the proposed antenna is very effective for point-to-point wireless communication systems, which need high-gain antennas with good impedance bandwidths. In addition, antenna covers are necessarily for outdoor applications.

REFERENCES

[1] K. Miura and M. Natori, "2-D array experiment on board a space flyer unit," *Space Sol. Power Rev.*, vol. 5, no. 4, pp. 345–356, 1985.
[2] S. Yao, X. Liu, and S. V. Georgakopoulos, "A mode reconfigurable Nojima origami antenna," in *Proc. IEEE Int. Symp. Antennas Propag. Soc. USNC/URSI Nat. Radio Sci. Meeting*, Oct. 2015, pp. 2237–2238.
[3] S. Yao, S. V. Georgakopoulos, B. S. Cook, and M. Tentzeris, "A novel reconfigurable origami accordion antenna," in *Proc. IEEE MTT-S Int. Microw. Symp.*, 2014, pp. 1–4.
[4] X. Liu, S. V. Georgakopoulos, and M. Tentzeris, "A novel mode and frequency reconfigurable origami quadrifilar helical antenna," in *Proc. IEEE 16th Annu. Wireless Microw. Technol. Conf.*, Cocoa Beach, FL, USA, 2015, pp. 1–3.
[5] S. Yao, X. Liu, S. V. Georgakopoulos, and M. M. Tentzeris, "A novel reconfigurable origami spring antenna," in *Proc. IEEE Antennas Propag. Soc. Int. Symp.*, 2014, pp. 374–375.
[6] S. Yao, X. Liu, J. Gibson, and S. V. Georgakopoulos, "Deployable origami Yagi loop antenna," in *Proc. IEEE Int. Symp. Antennas Propag. USNC/URSI Nat. Radio Sci. Meeting*, 2015, pp. 2215–2216.
[7] Z.-C. Ge, W.-X. Zhang, Z.-G. Liu, and Y.-Y. Gu, "Broadband and high-gain printed antennas constructed from Fabry–Perot resonator structure using EBG or FSS cover," *Microw. Opt. Technol. Lett.*, vol. 48, no. 7, pp. 1272–1274, 2006.
[8] P. L. Werner, Z. Bayraktar, B. Rybicki, D. H. Werner, K. J. Schlager, and D. Linden, "Stub-loaded long-wire monopoles optimized for high gain performance," *IEEE Trans. Antennas Propag.*, vol. 56, no. 3, pp. 639–644, Mar. 2008.
[9] Z. H. Jiang, Q. Wu, D. E. Brocker, P. E. Sieber, and D. H. Werner, "A low-profile high-gain substrate-integrated waveguide slot antenna enabled by an ultrathin anisotropic zero-index metamaterial coating," *IEEE Trans. Antennas Propag.*, vol. 62, no. 3. pp. 1173–1184, Mar. 2014.
[10] W. C. Yang, H. Wang, W. Q. Che, Y. Huang, and J. Wang, "High-gain and low-loss millimeter-wave LTCC antenna array using artificial magnetic conductor structure," *IEEE Trans. Antennas Propag.*, vol. 63, no. 1, pp. 390–395, Jan. 2015.
[11] L. Sang, Z. Wang, R. Xu, and B. Yan, "A compact high-gain patch antenna using stacked rings in LTCC technology," *J. Electromagn. Waves Appl.*, vol. 27, no. 3, pp. 330–337, 2013.
[12] G. Gnanagurunathan and K. Selvan, "Gain enhancement of microstrip patch antenna by using complementary EBG geometries," *J. Electromagn. Waves Appl.*, vol. 26, nos. 2/3, pp. 329–341, 2012.
[13] D. Kim and E. Kim, "A high-gain wideband antenna with frequency selective side reflectors operating in an anti-resonant mode," *IEEE Antennas Wireless Propag. Lett.,* vol. 14, pp. 442–445, 2015.
[14] Z. Hua, G. Haichuan, L. Hongmei, L. Beijia, L. Guanjun, and W. Qun, "A novel high-gain quasi-Yagi antenna with a parabolic reflector," in *Proc. Int. Symp. Antennas Propag.*, 2015, pp. 1–3.
[15] W. M. Haynes, *Handbook of Chemistry and Physics*, 91st ed. Boca Raton, FL, USA: CRC Press, 2011.
[16] X. Liu, S. Yao, B. S. Cook, M. M. Tentzeris, and S. V. Georgakopoulos, "An origami reconfigurable axial-mode bifilar helical antenna," *IEEE Trans. Antennas Propag.*, vol. 63, no. 12, pp. 5897–5903, Dec. 2015.